THE JOURNAL OF BIOLOGICAL CHEMISTRY
Vol. 279, No. 1, Issue of January 2, pp. 117–126, 2004

Printed in U.S.A.

Expression and Function of Gonadotropin-releasing Hormone (GnRH) Receptor in Human Olfactory GnRH-secreting Neurons

AN AUTOCRINE GnRH LOOP UNDERLIES NEURONAL MIGRATION*

Received for publication, July 22, 2003, and in revised form, September 18, 2003
Published, JBC Papers in Press, October 16, 2003, DOI 10.1074/jbc.M307955200

Roberto Giulio Romanelli‡, Tullio Barni§, Mario Maggi¶, Michaela Luconi¶, Paola Failli‖, Anna Pezzatini, Elisabetta Pelo‡‡, Francesca Torricelli‡‡, Clara Crescioli§§, Pietro Ferruzzi§§, Roberto Salerno§§, Mirca Marini**, Carlo Maria Rotella§§, and Gabriella B. Vannelli**¶¶**

*From the **Departments of Anatomy Histology and Forensic Medicine and Clinical Physiopathology and §§Endocrinology and ¶Andrology Unit and ‡‡Genetic Unit, Departments of ‡Internal Medicine and ‖Preclinical and Clinical Pharmacology, University of Florence, School of Medicine, Florence I-50134, Italy and §Department of Experimental and Clinical Medicine, University of Catanzaro, Catanzaro I-88100, Italy*

Olfactory neurons and gonadotropin-releasing hormone (GnRH) neurons share a common origin during organogenesis. Kallmann's syndrome, clinically characterized by anosmia and hypogonadotropic hypogonadism, is due to an abnormality in the migration of olfactory and GnRH neurons. We recently characterized the human FNC-B4 cell line, which retains properties present *in vivo* in both olfactory and GnRH neurons. In this study, we found that FNC-B4 neurons expressed GnRH receptor and responded to GnRH with time- and dose-dependent increases in GnRH gene expression and protein release (up to 5-fold). In addition, GnRH and its analogs stimulated cAMP production and calcium mobilization, although at different biological thresholds (nanomolar for cAMP and micromolar concentrations for calcium). We also observed that GnRH triggered axon growth, actin cytoskeleton remodeling, and a dose-dependent increase in migration (up to 3–4-fold), whereas it down-regulated nestin expression. All these effects were blocked by a specific GnRH receptor antagonist, cetrorelix. We suggest that GnRH, secreted by olfactory neuroblasts, acts in an autocrine pattern to promote differentiation and migration of those cells that diverge from the olfactory sensory lineage and are committed to becoming GnRH neurons.

The secretion of gonadotropin-releasing hormone (GnRH)[1] by GnRH neurons is vital for reproductive competence in all mammalian species. GnRH neurons are unique in that they arise from progenitor cells located outside of the central nervous system, in the olfactory placode. These neurons migrate through the nasal septum into the basal forebrain, where they establish their final scattered distribution within the septal and hypothalamic regions of the brain (1, 2). The mechanisms underlying the migration of the hypothalamic GnRH-producing neurons from the nasal region along the olfactory placode axons into the brain are still not fully understood. A detailed understanding of the process of GnRH migration clearly requires a complete cellular and molecular characterization of the GnRH neuron during early development. The physical migration of the GnRH neuron is well established. These cells migrate along olfactory axon bundles and reach the brain (nasal-forebrain junction). Recent studies (3, 4) highlight some trophic factors and potential guidance molecules that are involved in this process and that appear to play a role in the establishment and maintenance of the olfactory networks. Two immortalized GnRH-expressing neuronal cell lines, GT1 and GN, represent useful model systems for *in vitro* study of GnRH neuron biology. These cell lines have been isolated from tumors induced by genetically targeting the expression of the simian virus 40 large T antigen in mouse GnRH neurons (5, 6). Biochemical and functional studies have shown that these cells retain many characteristics of hypothalamic GnRH-secreting neurons (7–10). GT1 cells derived from postmigratory hypothalamic tumor (5), whereas GN neuronal cells have been isolated from olfactory bulb tumor of migration-arrested GnRH neurons (6). The different origin may be indicative of some different maturational stages of the two cell lines, as demonstrated by the fact that GT1 cells retain many characteristics of the mature hypothalamic GnRH neurons (7–10). On the contrary, it has been found recently (11, 12) that GN cells retain the characteristics of immature GnRH neurons and show high migratory activity *in vitro*. However, the factors that regulate the outgrowth and targeting of olfactory axons from the nose to the hypothalamus during embryogenesis have not yet been identified in humans. The GnRH-secreting neurons migrate across the nasal septum into the preoptic area, where they reside and project axons to the median eminence. Disruption of the migratory process, as expressed by olfactory axon targeting, is most likely a pathogenic factor for severe forms of reproductive dysfunctions and hypogonadotropic hypogonadism, such as Kallmann's syndrome (13). Kallmann's syndrome is considered a congenital form of hypogonadotropic hypogonadism. It is characterized by the association of an inability to smell (anosmia) with a defect in gonadal development due to GnRH deficiency (13–19). However, in humans, Kallmann's syndrome is characterized by considerable clinical and genetic heterogeneity. Some individuals with Kallmann's syndrome also display synkinesia, eye movement abnormalities, cerebellar dysfunction,

* This work was supported by grants from the Ministero dell'Istruzione, dell'Università e della Ricerca (MIUR) and from the University of Florence. The costs of publication of this article were defrayed in part by the payment of page charges. This article must therefore be hereby marked "*advertisement*" in accordance with 18 U.S.C. Section 1734 solely to indicate this fact.

¶¶ To whom correspondence should be addressed: Dept. of Anatomy Histology and Forensic Medicine, University of Florence, School of Medicine, V.le Morgagni 85, I-50134 Florence, Italy. Tel.: 39-55-410084; Fax: 39-55-4379500; E-mail: vannelli@unifi.it.

[1] The abbreviations used are: GnRH, gonadotropin-releasing hormone; RIA, radioimmunoassay; MA, monoclonal antibodies; RT, reverse transcription; GnRH-R, GnRH receptor; GAPDH, glyceraldehyde-3-phosphate dehydrogenase; BSA, bovine serum albumin; PTX, pertussis toxin; SFM, serum-free medium; TTBS, Tris transfer buffer saline.

gaze-evoked horizontal nystagmus, pes cavus, unilateral renal agenesia, and cleft palate (13, 18).

For the congenital forms of hypogonadotropic hypogonadism, the genes currently recognized are KAL and FGFR1, associated with Kallmann's syndrome; DAX 1, associated with adrenohypoplasia congenita; GnRH receptor, associated with resistance to GnRH therapy; and three loci also associated with obesity, leptin (OB), leptin receptor (DB), and prohormone convertase (PC1) (17, 19, 20). A less well characterized group of acquired hypogonadotropic hypogonadism encompasses a wide range of disorders such as infiltrative processes and space-occupying lesions, *i.e.* hemochromatosis, pituitary adenomas, and other tumors. Some forms of idiopathic hypogonadotropic hypogonadism, without an identifiable cause, develop after puberty, arising in sexually mature men. This adult-onset hypogonadotropic hypogonadism represents one of the few treatable forms of male infertility (15). Our contribution to clarify this complex biological problem has been to utilize the human GnRH-secreting neuronal cell line, FNC-B4 neurons (21–24). These primary long term cell cultures have been established, cloned, and propagated *in vitro* from human fetal olfactory epithelium (21). FNC-B4 cells expressed both neuronal proteins and olfactory genes and were responsive to odorant stimuli. They also maintained neuroendocrine properties. FNC-B4 neurons not only produced GnRH and responded to sex steroids, but they were sensitive to odorants in terms of GnRH production (22). In addition, endothelin-1 (23) and activin A (24), well known regulators of the GnRH-secreting neuron (25, 26), also modulated their secretory pattern. Thus, FNC-B4 cells with both olfactory and neuroendocrine characteristics, such as those that may occur in the human olfactory epithelium during organogenesis, provide an useful *in vitro* tool to study those factors potentially involved in olfactory or neuroendocrine phenotype commitment in humans.

In the current paper, a new role for GnRH is presented. GnRH can modulate the differentiation and migration of GnRH-secreting neurons, FNC-B4 cells, by receptor-mediated mechanisms.

EXPERIMENTAL PROCEDURES

Chemicals—GnRH (2200 Ci/mmol) was obtained from PerkinElmer Life and Analytical Sciences; the GnRH radioimmunoassay (RIA) kit was obtained from Buhlmann Laboratories AG (Allschwil, Switzerland). GnRH agonist buserelin (D-*tert*-butyl-Ser^6-des-Gly^{10}-Pro^9-ethylamide-GnRH) was purchased from Sigma. GnRH antagonist cetrorelix (Ac-D-Nal (2)1, D-Phe (4Cl)2, D-Pal (3)3, D-Cit6, D-Ala10) was purchased from ASTA Medica GmbH (Frankfurt, Germany).

Antisera—The following monoclonal antibodies (MA) were used for immunocytochemical or immunoblot analysis: mouse MA to human pituitary GnRH-R (F1G4), kindly provided by Dr. A. A. Karande, Department of Biochemistry, Indian Institute of Science, Bangalore, India (27); mouse MA to human vimentin (Vm; clone V9); mouse MA to human GAP43 (clone NCL-GAP43); and MA to human neurofilament 200 (NF200) (clone N52) were from Sigma; mouse MA to human actin (C-2) sc-8432 was from Santa Cruz Biotechnology, Inc. (Santa Cruz, CA); and mouse MA to human nestin (clone 10C2) was from Chemicon International Inc. (Temecula, CA). Other reagents were obtained at the highest grade available from commercial sources.

Cell Cultures—The primary neuroblast long term cell culture, FNC-B4, was established, cloned, and propagated *in vitro* from human fetal olfactory epithelium, as described previously (21). Although the cells have the some properties as those of immature neurons, they can differentiate and express neuronal markers and olfactory genes, as well as neuroendocrine characteristics (21–24). FNC-B4 cells, grown as a monolayer, are non-tumorigenic and have a normal human karyotype. FNC-B4 cells were cultured at 37 °C in 5% CO_2 in Coon's modified F-12 medium with 4.5 g/liter glucose, 10% fetal bovine serum (Laboratoires Eurobio, Les Ulis, France), antibiotic/antimycotic solution (penicillin, 100 IU/ml; streptomycin, 100 μg/ml). Coon's modified F-12 medium was purchased from Irvine Scientific (Santa Ana, CA).

Reverse Transcription (RT)-PCR Amplification—Total RNA was extracted from cultured cells using an RNeasy Midi Kit (Qiagen, Valencia, CA). Total RNA (500 ng) was retrotranscribed and then amplified using a Superscript One Step RT-PCR kit (Invitrogen). Specific oligonucleotide primers for the GnRH receptor (GnRH-R) mRNA were purchased from Invitrogen. The specific primers for human GnRH-R covered a 353-bp region of the human GnRH-R mRNA sequence, as deposited in the GenBank™ at NCBI (accession number NM_000406). The sequence of the sense primers was 5′-GTG TTG TGA AAG CCA GAC CA-3′. The sequence of the antisense primers was 5′-GTG GGA TGC TGT TGT TGA TG-3′. The contamination of genomic DNA was excluded by performing 35 cycles of amplification without retrotranscription. The integrity of the total RNA was verified by performing RT-PCR for the housekeeping gene, glyceraldehyde-3-phosphate dehydrogenase (GAPDH). The sequences of primers for GAPDH were: 5′-CCA TGG AGA AGG CTG GGG-3′ (sense) and 5′-CAA AGT TGT CAT GGA TGA CC-3′ (antisense) (28).

Real-time PCR—Primers and probes for β-actin and GnRH were as follows (Applied Biosystems, Foster City, CA): β-actin forward primer, 5′-TCACCCACACTGTGCCCATCTACGA-3′; reverse primer, 5′-CAGCGGAACCGCTCATTGCCAATGG-3′; the specific fluorescent probe, 5′-FAM-ATGCCCCCCCATGCCATCCTGCGTp-3′; GnRH forward primer, 5′-TGATTGTGCATTCATGTGCCT-3′; reverse primer, 5′-TCCACGCACGAAGTCAGTAGA-3′; the specific fluorescent probe for GnRH, 5′-FAM-AAGCCAATTCAAAAACTCCTAGCTGGCCTTAp-3′. Quantitative mRNA analysis was performed by simultaneous amplification of a target sequence, *i.e.* β-actin and GnRH, together with a housekeeping gene (GAPDH) (20× concentrated primer/probe mix, VIC®-labeled probe; Applied Biosystems, Foster City, CA). Probes were cleaved by the 5′-3′ exonuclease activity of *Taq* polymerase, allowing for the generation of target-specific fluorescence, followed and analyzed by real-time PCR assay in Micro-Amp optical 96-well plate using the automated ABI Prism 7700 Sequence Detector System (Applied Biosystems, Foster City, CA). The use of different labeled sets of probes allowed for the simultaneous analysis of several targets. GAPDH primers and probe concentrations have been lowered by Applied Biosystems to achieve the same C_t (cycle threshold) values obtained in the above single-plex PCR but lower R_n (fluorescence values); this ensured the ability of exactly quantifying target copy numbers without limiting the housekeeping (GAPDH) reaction. Real-time PCR was performed in a 25-μl final volume with 2× universal master mix, 1× GAPDH mix, 300 nM primer sets and 200 nM probes (either GnRH or β-actin), and 50 ng of cDNA. PCR was carried out with the following universal profile: 2 min at 50 °C (uracil-*N*-glycosylase activity), 3 min at 95 °C, 15 s at 95 °C, and 1 min at 60 °C for 40 cycles. Results were analyzed by ABI Prism Sequence Detection System software (version 1.7) (Applied Biosystems, Foster City, CA) and plotted by Microsoft Excel Software (Microsoft Excel Corp., New York, NY).

SDS-PAGE, Western Blot Analysis, and Immunoblotting—FNC-B4, DU145, HeLa, and LNCaP cells, grown to confluence, were scraped into phosphate-buffered saline (Ca^{2+}/Mg^{2+}-free), centrifuged, and resuspended in lysis buffer (20 mM Tris-HCl, pH 7.4, 150 mM NaCl, 0.25% Nonidet P-40, 1 mM Na_3VO_4, 1 mM phenylmethylsulfonyl fluoride, 1 mM EGTA). Protein concentration was measured according to Bradford (29) by the Coomassie Bio-Rad protein assay kit (Bio-Rad Laboratories). Aliquots containing 30 μg of proteins were diluted in 2× reducing Laemmli's sample buffer (62.5 mM Tris-HCl, pH 6.8, 10% glycerol, 1% SDS, 2.5% pyronin, and 100 mM dithiothreitol) and loaded onto 8 and 10% SDS-PAGE. After SDS-PAGE, proteins were transferred to nitrocellulose membranes (Immobilon-P transfer membranes polyvinylidene difluoride; Millipore®, Bedford, MA). Membranes were blocked overnight at 4 °C in 5% BSA-TTBS buffer (0.1% Tween 20, 20 mM Tris-HCl, 150 mM NaCl), washed in TTBS, and incubated for 2 h with primary antibodies (F1G4 antibody 1:2000; anti-actin antibody 1:500; anti-nestin antibody 1:500) diluted in 2% BSA-TTBS, followed by peroxidase-conjugated secondary IgG (Sigma). Finally, the reacted proteins were revealed by the enhanced chemiluminescence system (ECL; Roche Diagnostics).

Binding Studies—Binding studies were performed as described previously (23). Confluent FNC-B4 cells were washed once with 20 mM HEPES, 10 mM $MgSO_4$, 0.5% BSA, pH 7.4, and incubated in 200 μl of the same binding medium at 22 °C for 60 min with fixed concentrations (15–50 pM) of [^{125}I]GnRH in the presence or absence of increasing concentrations of unlabeled GnRH (10^{-11}-10^{-7} M). After incubation, the cells were washed extensively using ice-cold phosphate-buffered saline, 0.1% BSA, solubilized in 0.5 N NaOH, and the cell-bound radioactivity was determined. Measurements were obtained in triplicate. Cell counts routinely varied by less than 10% in each of the wells.

GnRH RIA—Immunoreactive GnRH was extracted from conditioned media of FNC-B4 cells with chilled absolute ethanol (−20 C°), evaporated to dryness, and subjected to RIA using a commercial kit (Buhlmann Laboratories AG, Allschwil, Switzerland), as described previ-

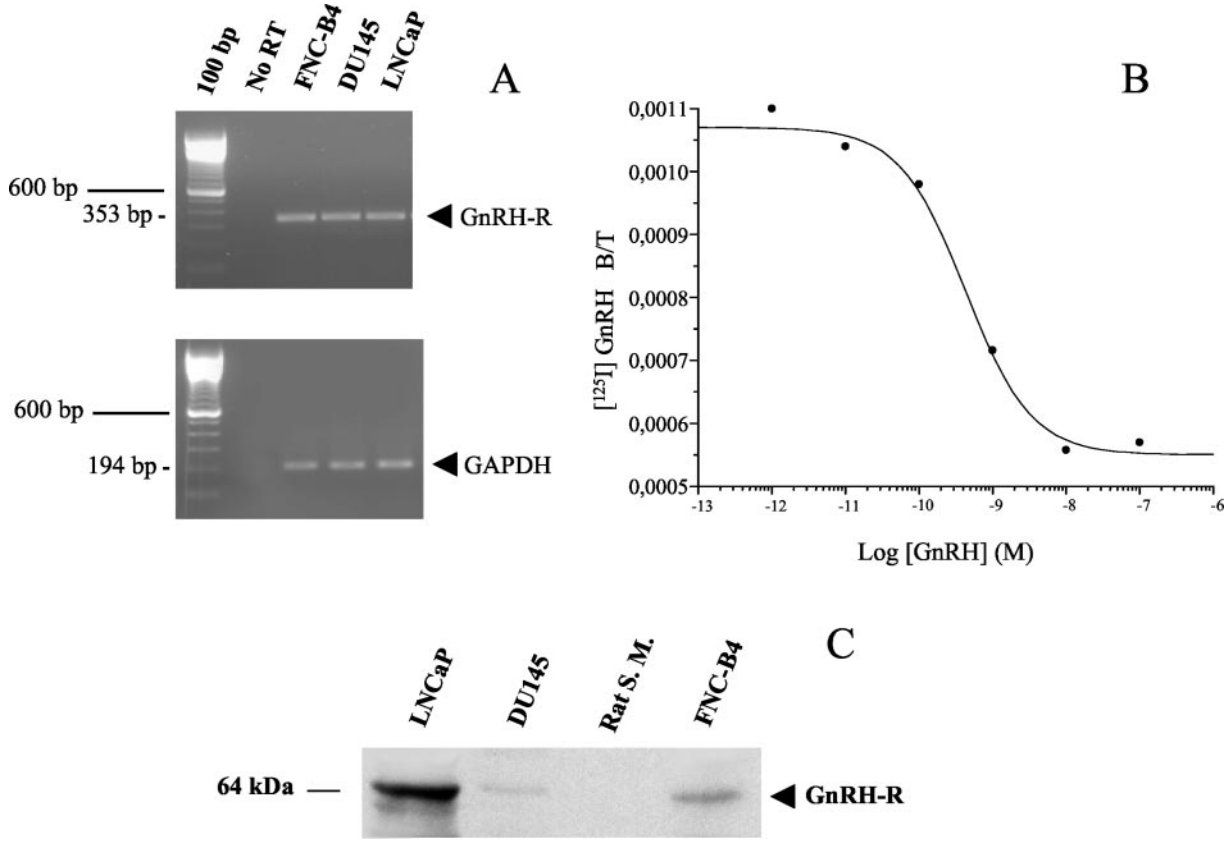

FIG. 1. **GnRH receptor expression in human FNC-B4 cell line.** *Panel A*, RT-PCR amplification. Human FNC-B4 cells express the GnRH receptor. 500 ng of total RNA were retrotranscribed and then amplified by PCR with primers specific for GnRH-R (*lane 3*). *Lane 1*, molecular weight marker ϕX 174/HaeIII. *Lane 2*, the reaction was also run with a template derived from a retrotranscription carried out with no RNA (control reaction). *Lanes 4* and *5*, amplified bands of DU145 and LNCaP cell lines as positive controls. GAPDH gene expression is also shown as a control (*GAPDH*; 194 bp). Note the presence of signals of the expected size (*GnRH*; 353 bp) in FNC-B4 cells. *Panel B*, binding studies. Competition curve for [^{125}I]GnRH with unlabeled GnRH (10^{-12}–10^{-7} M). Mathematical analysis of four different homologous completion curves (LIGAND program) revealed that FNC-B4 cells express a single class with high affinity (K_d = 1.17 ± 0.6 nM) and low capacity (2,775 ± 441 sites/cell) binding sites. *Panel C*, Western blot analysis. Western blot analysis of total lysates from LNCaP, DU145, rat skeletal muscle, and FNC-B4 cells with the monoclonal antibody F1G4 against GnRH-R. Lysates were obtained as described under "Experimental Procedures," and protein extracts were separated onto 8% reducing SDS-PAGE. Western blot analysis with F1G4 antibody (1:2000 dilution) revealed a single protein band indicated by the *arrow* migrating at the expected molecular size (*64 kDa*). LNCaP and DU145 cells were used as positive controls, whereas rat skeletal muscle was used as negative control.

ously (22). Before extraction, the recovery of unlabeled GnRH added to the media was 81%. A close parallelism with the standard curve was found when serial dilution of FNC-B4 cell conditioned media or extracts of the arcuate nucleus of the rat hypothalamus were subjected to RIA.

Digital Video Imaging of Intracellular Free Calcium—Digital video imaging of the intracellular-free calcium concentration ($[Ca^{2+}]_i$) in individual human FNC-B4 cells was performed as described previously (30). Human neurons were grown to subconfluence in complete culture medium on round glass coverslips (25-mm diameter, 0.2-mm thick) for 72 h and then incubated for 48 h in serum-free medium. Cells were then loaded with 10 μmol/liter Fura-2/AM and 15% Pluronic F-127 for 30 min at 22 °C. $[Ca^{2+}]_i$ was measured in Fura-2-loaded cells in HEPES-$NaHCO_3$ buffer containing 140 mmol/liter NaCl, 3 mmol/liter KCl, 0.5 mmol/liter NaH_2PO_4, 12 mmol/liter $NaHCO_3$, 1.2 mmol/liter $MgCl_2$, 1.0 mmol/liter $CaCl_2$, 10 mmol/liter HEPES, and 10 mmol/liter glucose, pH 7.4. Ratio images (340/380 nm) were collected every 3 s, and calibration curves were obtained for each cell preparation (30). GnRH or an analog (buserelin) (from 10 μM to 100 nM) were added directly to the perfusion chamber immediately after recording the $[Ca^{2+}]_i$ basal value. In parallel experiments, cells were preincubated with 0.1–1 μM cetrorelix for 10 min before the addition of GnRH or buserelin.

cAMP Determination—Cells were plated in 24-well plates and grown to subconfluence in Coon's modified F-12 medium with 10% fetal calf serum. After removing the medium, cells were incubated for 20 min at 37 °C in assay buffer (0.025 mol/liter Tris acetate, 0.25 mol/liter sucrose, 0.5% BSA, 5 mmol/liter glucose, and 0.6 mmol/liter 3-isobutyl-1-methylxanthine) in the presence or absence of increasing concentrations of buserelin or GnRH. Experiments were also performed by incubating FNC-B4 cells with a fixed (1 μM) concentration of cetrorelix. To stop the reaction, equal volumes of cold (−20 °C) absolute ethanol were added, and samples were reconstituted with 50 mmol/liter sodium acetate, pH 6.2, after vacuum drying. cAMP was determined in 100-μl aliquots of the supernatant using both an enzyme immunoassay kit (EIA system; Amersham Biosciences) and an RIA kit (PerkinElmer Life and Analytical Sciences) as described previously (21). Protein was determined by a BCA protein assay kit (Pierce) with bovine BSA as standard. All assays were performed in duplicate.

Immunofluorescence and Confocal Laser Microscopy—FNC-B4 cells were cultured on glass coverslips in serum-free medium for 18 h and then left untreated or incubated with GnRH or buserelin. Cells were then fixed with paraformaldehyde 3.7%, pH 7.4, for 10 min and then permeabilized for 10 min with phosphate-buffered saline (Ca^{2+}/Mg^{2+}-free) containing 0.1% Triton X-100. Immunostaining was performed as described previously (21) using anti-vimentin (1:100), anti-GAP43 (1:50), anti-neurofilament (1:200), anti-actin (1:100), and anti-nestin (1:200) antibodies, followed by A-11001 Alexa Fluor 488 goat anti-mouse IgG(H+L) conjugate (1:200) antibody (Molecular Probes, Eugene, OR). F-actin was stained with rhodamine phalloidin (1:50) (Molecular Probes, Eugene, OR) in the permeabilization solution for 45 min at room temperature. Cells were viewed with a laser scanner confocal microscope (MRC 600; Bio-Rad Laboratories) equipped with a Nikon diaphot inverted microscope or with Nikon Microphot-FX microscope (Nikon, Tokyo, Japan).

Chemotactic Assay—Cell migration was carried out as described previously (31). Briefly, modified Boyden chambers (Nuclepore Inc., Pleasanton, CA), equipped with a 13-mm diameter and an 8-μm porosity polyvinylpyrrolidone-free polycarbonate filters were used; the filters were coated with 20 μg/ml human type I collagen (Collaborative Biomedical Products, Bedford, MA) for 30 min at 37 °C. Confluent FNC-B4 cells were incubated in serum-free medium for 24 h and then treated

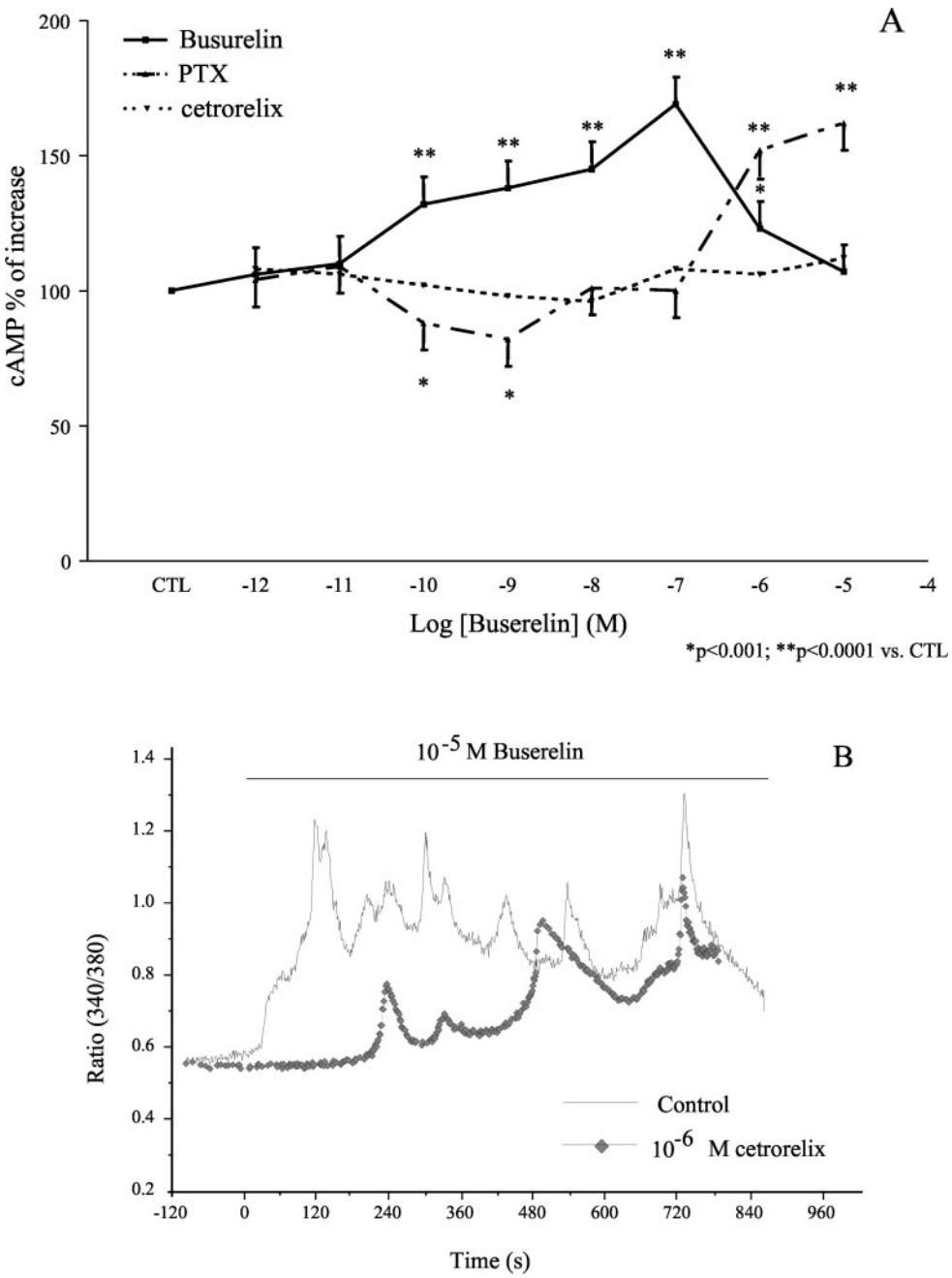

FIG. 2. **Intracellular signaling activated by GnRH in FNC-B4 neurons.** *Panel A*, increase in intracellular cAMP. cAMP accumulation in FNC-B4 cells stimulated with increasing concentrations of GnRH analog buserelin (10^{-12}–10^{-5} M; *solid line*) alone or in the presence of PTX (100 ng/ml; *dashed line*) or cetrorelix (10^{-7} M; *dotted line*). A short term (20 min) incubation time of FNC-B4 cells with buserelin induced a significant dose-dependent (EC_{50} = 0.25 nM) and biphasic cAMP response. Although low doses of buserelin (10^{-10}–10^{-7} M) induced a significant increase in cAMP accumulation, as compared with control, higher concentrations (10^{-6}–10^{-5} M) failed to increase cAMP levels. Simultaneous presence of PTX or cetrorelix abolished buserelin stimulatory effect. Results are expressed as percent (mean ± S.E.) increase over the control in six different experiments. *, $p < 0.001$ and **, $p < 0.0001$ *versus* control (*CTL*). *Panel B*, effects of buserelin on cytosolic calcium concentration. Typical time course of buserelin effect on intracellular calcium concentration (fluorescence ratio) of Fura-2-loaded FNC-B4 cells. The *panel* shows the average of the measurements obtained in the analyzed cells (n = 30). Buserelin (10^{-5} M) induced an increase in intracellular calcium level in Fura-2-loaded FNC-B4 cells; cetrorelix (10^{-6} M) abolished this stimulatory effect.

with increasing concentrations of GnRH or buserelin, in the presence or absence of cetrorelix used at 10^{-7} M and pertussis toxin (PTX; 100 ng/ml). After mild trypsinization with 0.05% trypsin-EDTA, a 210-μl aliquot, corresponding to 4×10^4 cells/Boyden chamber, was added to the top wells and incubated at 37 °C in 5% CO_2 for 6 h. After incubation, the migrated cells were fixed in 96% methanol and stained with Harris' hematoxylin solution. Chemotaxis was quantitated by counting six randomly chosen fields per filter, and results were expressed as the number of cells/high power field.

Statistical Analysis—Statistical analysis was performed by one-way or two-way analysis of variance, followed by Duncan's test and by unpaired and paired Student's t test, with the level of $p < 0.05$ accepted as statistically significant. The computer program ALLFIT was used for the analysis of sigmoidal dose-response curves (32). The binding data were evaluated quantitatively with nonlinear least square curve fitting using the computer program LIGAND (33).

RESULTS

GnRH-R Expression in Human FNC-B4 Cell Line—As shown in Fig. 1, FNC-B4 cells expressed both the gene and protein for GnRH-R. RT-PCR studies indicated transcripts of the expected size (*panel A*). In *panel B*, data from binding experiments are reported. Mathematical analysis of four dif-

ferent homologous competition curves for GnRH (LIGAND program) revealed that FNC-B4 cells express a single class with high affinity (K_d = 1.17 ± 0.6 nM) and low capacity (2,775 ± 441 sites/cell) binding sites. Western blot analysis (*panel C*) of protein lysates from FNC-B4 cells confirmed GnRH-R presence at the expected molecular mass (64 kDa). LNCaP and DU145 cells and rat skeletal muscle (34) have been used as positive and negative controls, respectively.

Intracellular Signaling Activated by GnRH in FNC-B4 Neurons—Exposure of FNC-B4 cells to increasing concentrations of GnRH (from 10^{-12} to 10^{-5} M) or buserelin for 20 min caused dose-dependent and biphasic cAMP responses (Fig. 2*A*). Nanomolar GnRH concentrations caused a progressive increase in cAMP production (1.7-fold; EC_{50} = 0.25 nM). Conversely, micromolar concentrations (10^{-6} and 10^{-5} M) failed to increase cAMP levels. This failure was completely prevented by pretreatment with PTX (100 ng/ml). Cetrorelix (10^{-7} M), a GnRH-releasing hormone antagonist, was able to abolish GnRH-induced cAMP increase. Using computerized image analysis, we also tested the effects of increasing concentrations of GnRH and GnRH analogs on cytosolic calcium concentration in Fura-2-loaded FNC-B4 cells. Only high micromolar concentrations (10^{-5} M) of GnRH (not shown) or buserelin elicited bell-shaped intracellular calcium responses. This stimulatory effect was blunted by incubation with cetrorelix (10^{-6} M) (Fig. 2*B*).

Biological Effects of GnRH via Autocrine Loop in FNC-B4 Neurons—After 24 h of exposure to GnRH or buserelin (10^{-7} M), FNC-B4 cells changed their polyedric shape (Fig. 3) and acquired a spindle-shape morphology that was accompanied by increased of axons growth and actin cytoskeletal remodeling to a motile phenotype. In particular, GnRH exposure induced the development of macropinocytic structures, broad lamellae, and numerous microspikes, as detected by immunofluorescence staining using antibody against actin (Fig. 4*A*, *upper panels*). These different cell protrusions were readily visualized by staining cellular filamentous actin (Fig. 4*A*, *lower panels*). Unstimulated FNC-B4 cells showed an intense actin stress fiber network; in this assay, these cells displayed actin cytoskeletal remodeling (12 ± 2%, n = 5). Exposure to GnRH caused various morphologies of actin-based cell deformations, *i.e.* actin patches, filopodia, lamellipodia, and membrane ruffles (80 ± 3% of FNC-B4 cells, n = 5, $p < 0.001$ *versus* untreated cells). Cetrorelix (100 nM) was able to significantly decrease GnRH-induced modifications (22 ± 2%, n = 3, $p < 0.001$ *versus* GnRH-treated cells). These changes in cell shape were parallel to a time-dependent increase (up to 24 h) of both mRNA levels of actin (Fig. 4*B*) ($p < 0.001$ *versus* control) and protein expression (Fig. 4*C*). To identify the developmental markers critical for tracing cues, important for GnRH cell differentiation, we also evaluate nestin expression, commonly used to characterize developing neurons that are present in proliferating neuronal precursor cells; this molecule is usually down-regulated upon differentiation (35). Immunofluorescence analysis using a monoclonal antibody against nestin indicated that FNC-B4 cells expressed nestin (Fig. 5, *panel A*). Exposure to GnRH (10^{-7} M and 10^{-6} M) for 24 h, as evaluated by Western blot analysis of FNC-B4 cell lysates, down-regulated nestin expression (Fig. 5, *panel B*). To verify the presence of a functional autocrine feedback loop for GnRH in the FNC-B4 cells, we stimulated cells with native GnRH and/or with the GnRH agonist, buserelin. Real time PCR for GnRH showed a time-dependent up-regulation of the gene (Fig. 6, *panel A*). RIA studies indicated that GnRH release was affected positively by GnRH-R stimulation. Indeed, buserelin, recognizable in our GnRH RIA only in micromolar concentrations (IC_{50} = 3.57 ± 2 μM), stimulated GnRH secretion by the FNC-B4 cells (EC_{50} = 27 ± 18 nM, n = 3). This stimulatory effect of buserelin on GnRH secretion was completely blunted by simultaneous incubation with an equimolar concentration (100 nM) of a GnRH antagonist, cetrorelix (Fig. 6, *panel B*).

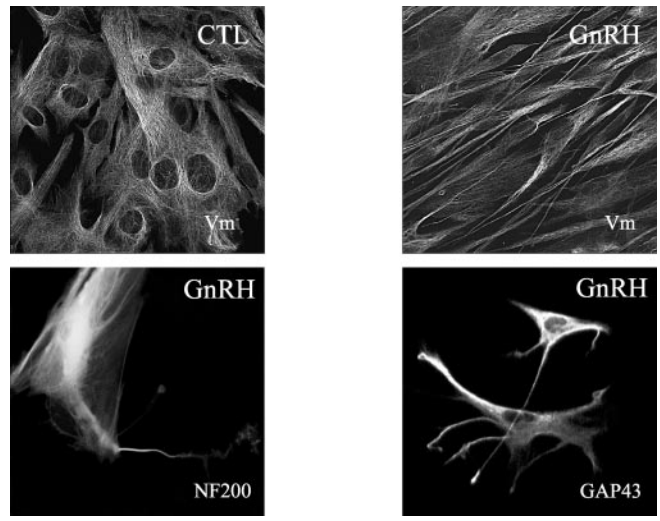

FIG. 3. **Cell shape modifications after stimulation with GnRH in FNC-B4 cells.** FNC-B4 cells were cultured on glass coverslips in serum-free medium for 18 h and then left untreated or incubated with GnRH (10^{-7} M). Cells were stained for indirect immunofluorescence using the mouse MA against human vimentin (*Vm*) (clone V9) as primary antibody (1:100), followed by A-11001 Alexa Fluor 488 goat anti-mouse IgG(H+L) conjugated (1:200) antibody. Cells were then viewed with a laser scanner confocal microscope (original magnification, ×200). Note, in the presence of GnRH, that cells changed their polyedric shape and acquired a marked spindle-shape morphology, accompanied by increased length and ramifications of cytoplasmic processes. By using either a mouse MA against human neurofilament 200 (*NF200*) (clone N52) as primary antibody (1:200) or a mouse MA against human GAP43 (clone NCL-GAP43) (1:50), cells viewed with a Nikon Microphot-FX microscope (original magnification, ×150; Nikon, Tokyo, Japan) showed neurofilaments extended only in the region of the growth cone (*NF200*), whereas microtubules extended further, filling the lamellae and occasionally entering one or two filopodia (*GAP43*).

Migration Assay—Because FNC-B4 cells were established from early gestational fetal explants, we hypothesized that they most probably retained migratory potentials. To address this issue, a Boyden chamber technique was utilized to test chemotaxis (migration of cells toward regions at higher concentration of the chemotactic factors). As expected, FNC-B4 neuronal cells were intrinsically migratory. This cell line responded to serum-free medium (SFM) conditions, demonstrating a time-dependent increase in spontaneous random migration (6 ± 1.5 cells/high power field after 6 h of incubation, 10 ± 3.2 cells/high power field after 12 h of incubation; n = 20). Moreover, an overt migratory pattern was observed in response to chemoattractants. Therefore, we investigated whether GnRH receptor signaling was also required for cell motility. As shown in Fig. 7, *panels A* and *B*), GnRH and buserelin were able to induce a migratory pattern in the FNC-B4 cells. In particular, a dose-dependent pattern was observed by employing different concentrations of GnRH (from 10^{-11} to 10^{-7}) (n = 8; *, $p < 0.005$ *versus* SFM; #, $p < 0.05$ *versus* lower dose) (Fig. 7, *panel A*). Cetrorelix (10^{-7} M) was able to counteract both GnRH and buserelin effects (Fig. 7, *panels A* and *B*). To investigate whether the $G_{i/o}$ protein family was involved down-stream of receptor activity, the sensitivity of this cell line to PTX was evaluated. Therefore, FNC-B4 cells were pre-treated with 100 ng/ml PTX for 16 h and then stimulated with GnRH (10^{-6} or 10^{-7} M) or buserelin (data not shown) for 6 h. Pre-incubation with PTX reduced GnRH-induced migration significantly (n = 3; *, $p < 0.005$; #, $p < 0.05$ *versus* SFM) (Fig. 7, *panel B*).

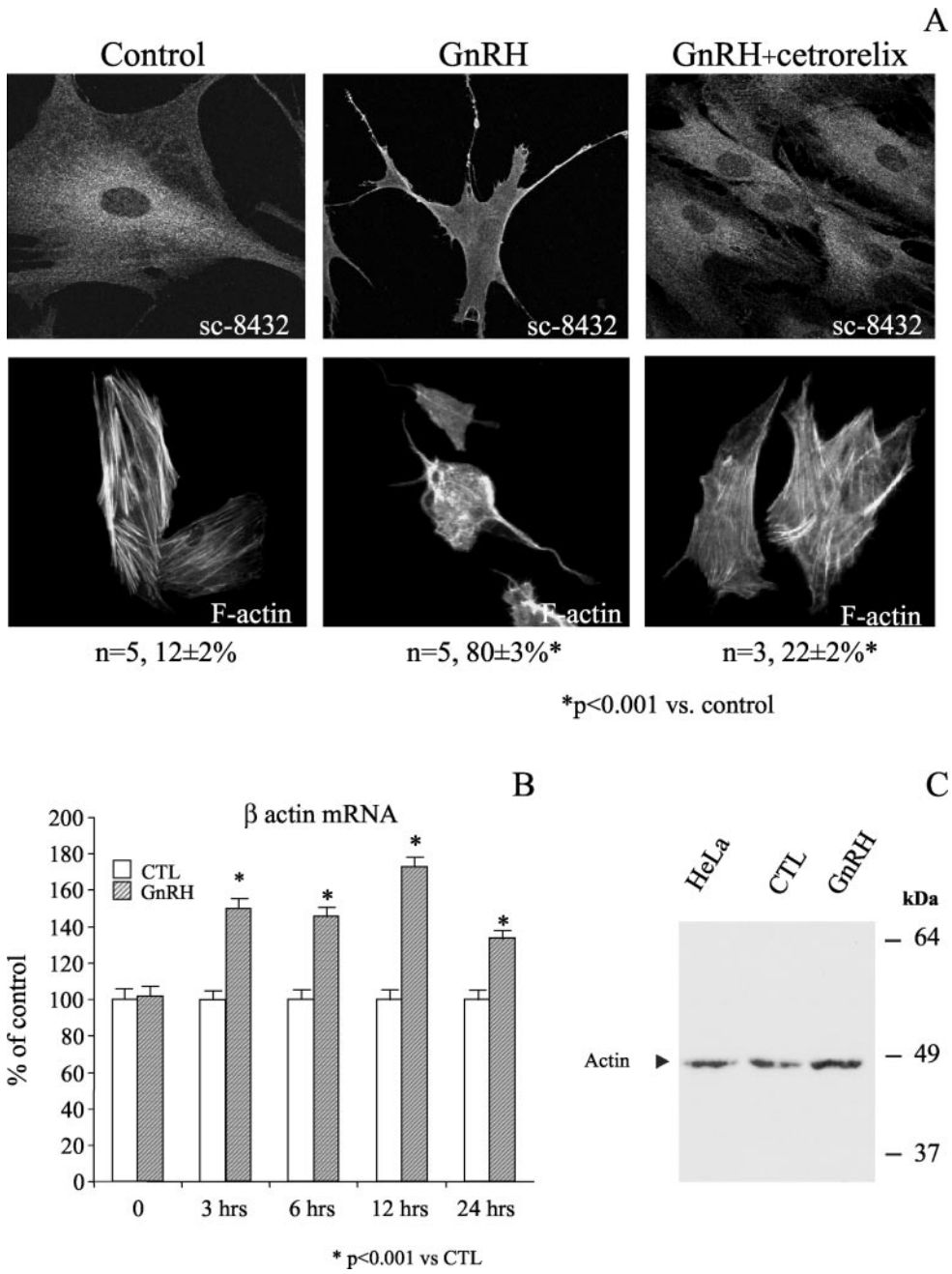

FIG. 4. *Panel A*, actin remodeling after stimulation with GnRH in FNC-B4 cells. FNC-B4 cells were cultured on glass coverslips in serum-free medium for 18 h and then left untreated or incubated with GnRH (10^{-7} M). Cells were stained for indirect immunofluorescence using the mouse MA against actin (C-2) sc-8432 as primary antibody (1:100). A-11001 Alexa Fluor 488 goat anti-mouse IgG(H+L) conjugated (1:200) antibody was used as secondary antibody. Cells were viewed with a laser scanner confocal microscope (*sc-8432*) (original magnification, ×300). Note, in the presence of GnRH, the marked spindle-shape morphology accompanied by membrane protrusions, such as microspikes and growing filaments. In the *lower panels*, F-actin, following fixation, was visualized with rhodamine phalloidin (1:50) in the permeabilization solution for 45 min at room temperature. Cells were then viewed with a Nikon Microphot-FX microscope (original magnification, ×150; Nikon, Tokyo, Japan). Note that control cells showed a marked actin stress fiber network. After GnRH exposure, cells displayed various morphologies of actin-based cell deformations, *i.e.* actin patches, filopodia, lamellipodia, and membrane ruffles. Cetrorelix (10^{-7} M) was able to significantly blunt these GnRH-induced morphological features. *Panel B*, time course real time PCR for β-actin in FNC-B4 cells. Quantitative mRNA analysis was performed by simultaneous amplification of the target sequence β-actin together with a housekeeping gene (GAPDH) in FNC-B4 cells stimulated with GnRH (10^{-7} M) for 3, 6, 12, and 24 h. Results are expressed as percent increase over control (GAPDH gene) values. Note that the time course expression revealed a significant increase in mRNA levels starting from the 3rd h (*, $p < 0.001$ *versus* control). *Panel C*, expression of actin protein in FNC-B4 cells. Western blot analysis of total lysates from FNC-B4 cells with anti-actin (C-2) sc-8432 antibody after 24 h of stimulation with GnRH (10^{-7} M). Thirty micrograms of cell lysates were separated onto 10% reducing SDS-PAGE. HeLa cells were used as positive control. Western blot analysis with anti-actin antibody (1:500) revealed a single protein band (43 kDa) indicated by the *arrowhead* migrating at the expected molecular mass. Molecular mass markers are indicated to the *right* of the blot. Quantification of bands corresponding to actin protein in Western blots was made directly on the films by image scanning analysis using Photoshop 5.5 software. Data have been reported as mean ± S.E. of percentage increase over control taken as 100%: *CTL* = 100 ± 16.9, *GnRH* = 142.2 ± 3.3, *HeLa* = 124.4 ± 5.2 ($n = 3$, $p < 0.05$ GnRH *versus* CTL).

DISCUSSION

This study provided the first evidence that GnRH is able to induce both differentiation and migration of human olfactory GnRH-secreting neurons through a receptor-mediated mechanism. In adult life, the olfactory neurons reside within the nasal cavity, and the GnRH cells dwell within the hypothala-

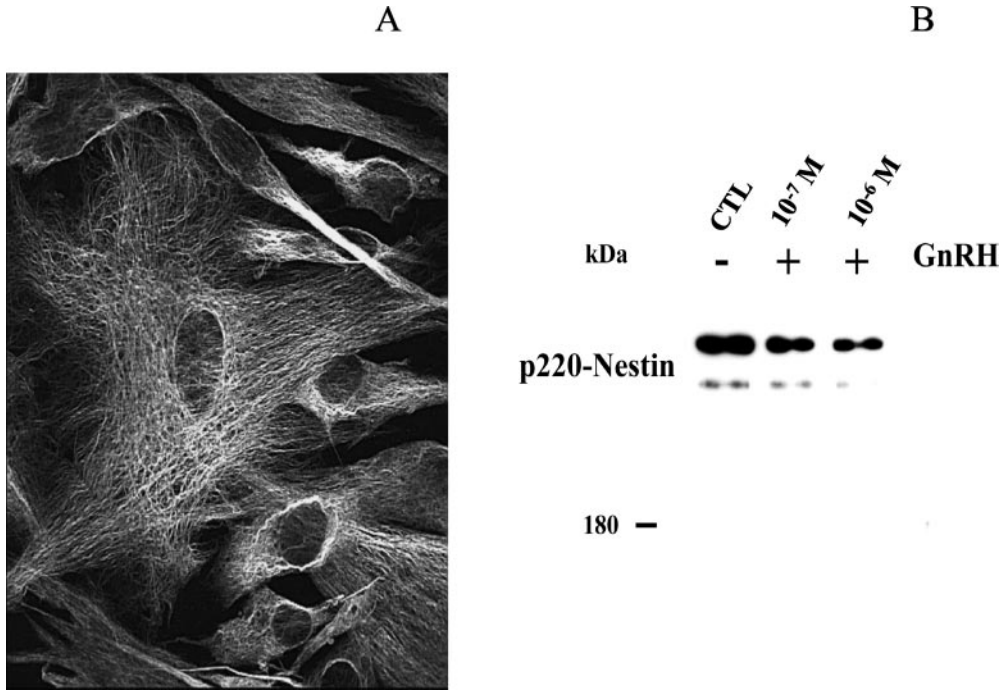

FIG. 5. *Panel A*, nestin expression in FNC-B4 cells. FNC-B4 were stained with anti-nestin antibody (clone 10C2) as primary antibody (1:200). A-11001 Alexa Fluor 488 goat anti-mouse IgG(H+L) conjugated (1:200) antibody was used as secondary antibody. Cells were viewed with a laser scanner confocal microscope (original magnification, ×200). Note the high constitutive expression of this protein by FNC-B4 cells. *Panel B*, modulation of nestin expression by GnRH in FNC-B4 cells. Western blot analysis of total lysates from FNC-B4 cells untreated (*CTL*) or following 24 h of incubation with GnRH (10^{-7}–10^{-6} M). Thirty micrograms of cell lysates were separated onto 6% reducing SDS-PAGE. Western blot analysis with anti-nestin antibody (clone 10C2) (1:1000) revealed a double band migrating approximately at the expected 220-kDa molecular mass. Note the decreased expression of nestin in respect to GnRH dose.

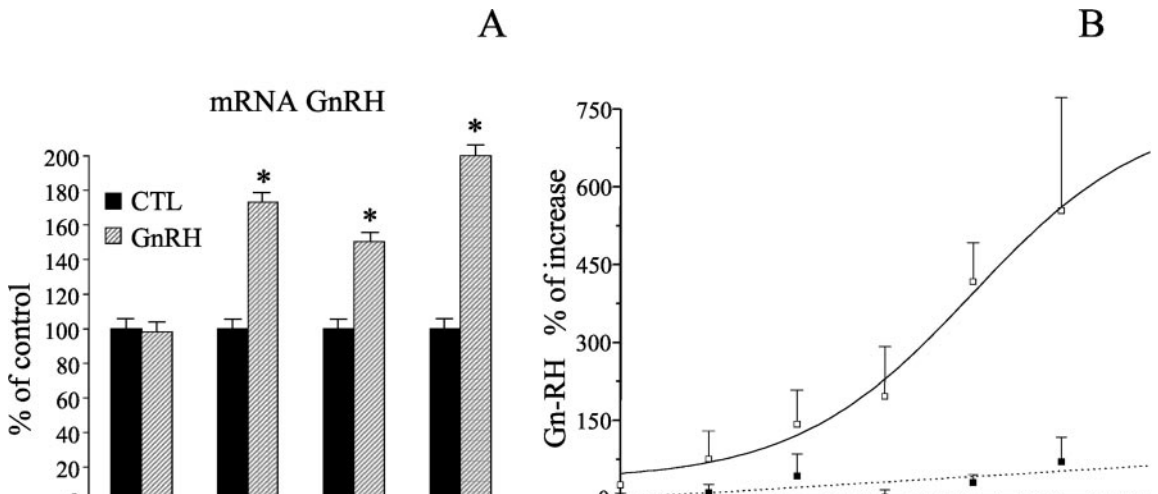

FIG. 6. *Panel A*, time course quantitative real-time PCR for the GnRH gene in FNC-B4 cells. Quantitative mRNA analysis was performed by simultaneous amplification of the target sequence GnRH together with a housekeeping gene (GAPDH) in FNC-B4 cells treated with GnRH (10^{-7} M) for 3, 12, and 24 h. Results are expressed as % increase over control (GAPDH gene) values. Note that the time course expression revealed a significant increase in mRNA levels starting from the 3rd h (*, $p < 0.001$ *versus* control). *Panel B*, effect of agonist buserelin on GnRH secretion. Results are expressed as percent increase over the control value (100%) of GnRH secretion by FNC-B4 cells stimulated with increasing concentrations of buserelin (10^{-12}–10^{-7} M) without (*open squares*) or with (*filled squares*) cetrorelix (10^{-7} M). In the absence of cetrorelix, buserelin induced a 4- to 5-fold increase in GnRH secretion. The stimulatory effect was almost completely abolished by cetrorelix.

mus. During development, both the olfactory and GnRH neurons originate in the olfactory placode. Olfactory neuronal precursors divide and differentiate in the nose, where they establish central and peripheral connections responsible for transmitting chemosensory information to the brain. In the meanwhile, GnRH neuroblasts emigrate from their birthplace, the nose, and proceed along characteristic pathways to reach the hypothalamus to establish contact with the portal vessels. In humans, the olfactory epithelium has been considered unable to maintain multipotent-olfactory or neuroendocrine-stem cell populations throughout life. However, the recent discovery of neural progenitor cells in the subcortical white matter of the adult human brain indicates that postnatal neurogenesis might be a potential mechanism by which the nervous system

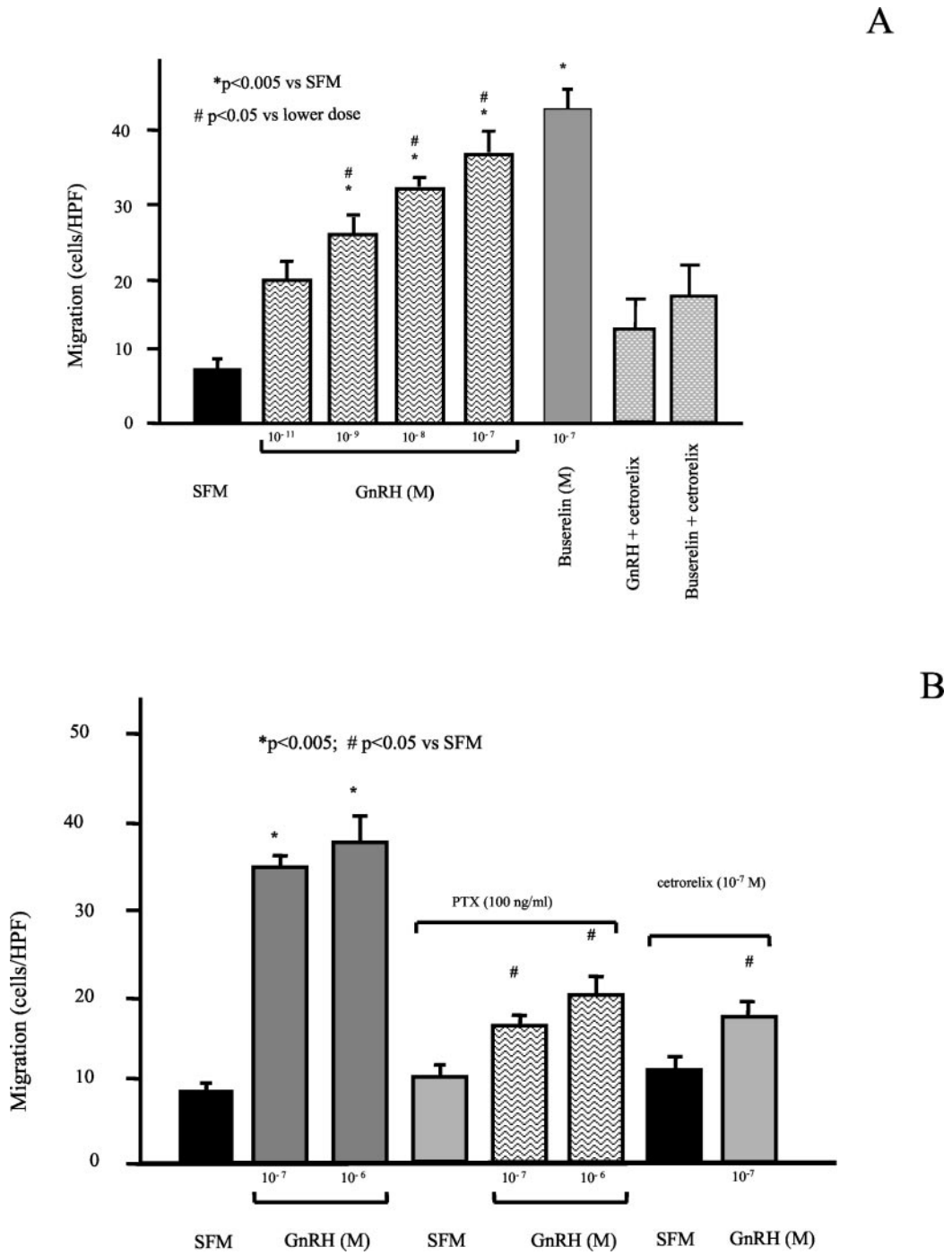

FIG. 7. *Panel A*, migration assay. Chemotactic response of FNC-B4 cells cultured for 24 h in SFM before migration. This assay was performed using modified Boyden's chambers in the absence or presence of increasing concentrations of GnRH. Results are expressed as mean ± S.D., deriving from experiments performed in triplicate. *, $p < 0.005$ *versus* control (*SFM*); #, $p < 0.05$ *versus* lower dose (10^{-11} M). Note the dose-dependent GnRH-induced increase (3–4-fold increase) in cell migration. Buserelin (10^{-7} M), a GnRH analog, also induced a significant cell migration (*, $p < 0.005$). Cetrorelix (10^{-7} M) blocked GnRH- and buserelin-induced chemotaxis. *Panel B*, chemotactic response of FNC-B4 cells cultured for 24 h in SFM before the chemomigration assay. This assay was performed using modified Boyden's chambers, in the absence or presence of increasing concentrations of GnRH and PTX (100 ng/ml); cetrorelix was used at 10^{-7} M. Results are expressed as mean ± S.D. from triplicate experiments. *, $p < 0.005$ and #, $p < 0.05$ *versus* control (*SFM*).

repopulates certain neuronal lineage (36). Thus, FNC-B4 cells, retaining properties of both olfactory and GnRH neurons, provided a human model system to study the role of GnRH on neuronal commitment. We demonstrated previously (22–24) that FNC-B4 cells release authentic GnRH in response to various stimuli. The present study showed that FNC-B4 cells expressed both gene and protein for GnRH-R and that its activation led to GnRH up-regulation at gene and protein levels. In fact, exposure of FNC-B4 cells to GnRH triggered a dose-dependent increase in GnRH release. Expression of GnRH-R has been found in cultured hypothalamic cells and tissue from fetuses and adult animals with similar characteristics to those found in both the pituitary gland and pituitary cells (37, 38). Expression of GnRH-R in hypothalamic GT1 neurons provided the physiological basis for a number of earlier observations on the control of GnRH secretion. The ability of GT1 cells to establish episodic GnRH release in the absence of other cell types indicates that intrinsic autocrine factors may

be important for its pulsatile release (39, 40). Our results in human olfactory FNC-B4 cells are in agreement with those of the aforementioned studies. They suggest that in humans a positive ultrashort autocrine loop contributes to regulate GnRH secretion. GnRH signals are transmitted via a specific cell surface receptor, a member of the G protein-coupled receptor superfamily (37, 38). The exposure of FNC-B4 cells to GnRH caused an increase in cAMP production and mobilization of intracellular calcium stores, although at different concentrations. Indeed, low GnRH concentrations stimulated cAMP production, whereas higher concentrations caused an increase in intracellular calcium and a lack of cAMP stimulation. This latter effect was reverted by PTX. We therefore concluded that, in FNC-B4 neuroblasts, GnRH-R is also coupled both to stimulatory and inhibitory G proteins. GnRH-R have been reported to couple to G_s in primary pituitary cultures and in pituitary derived GCH3 cells. This G protein activates adenylate cyclase, cAMP production, and protein kinase A activation (41, 42). Antiproliferative signaling of GnRH in human reproductive tract tumors is mediated through the PTX-sensitive G_i protein (43, 44). Moreover, recent research has demonstrated that, in GT1 cells, GnRH-modulated neuronal Ca^{2+} signaling occurs also via G_i inhibitory mechanisms (45). Our findings in human olfactory neurons suggest that GnRH, according to its concentration, is able to switch the coupling of GnRH-R to specific G proteins and thus to regulate distinct biological responses (46). In this study we also showed that GnRH signaling induced growth cones extending and actin cytoskeletal remodeling to a motile cell phenotype (47). In particular, GnRH stimulated both morphological modifications of cell shape and development of membrane ruffles, filopodia, and lamellipodial extension, as well as an increase in gene and protein expression of actin. Furthermore, increasing GnRH concentrations stimulated cell migration in a dose-dependent manner. A specific GnRH receptor antagonist blocked the migratory promoting activity of GnRH. Moreover, the fact that PTX pretreatment was able to reduce GnRH-dependent migration in a dose-dependent manner suggests that these effects were coupled to PTX-sensitive $G_{i/o}$ proteins (43–45). Several factors, including anosmin-1 (48), NELF (3), the receptor tyrosine kinase Ark (11), and FGFR1 (20), have been described as playing a role in some aspects of GnRH cell migration. However, to our knowledge, this is the first report on GnRH-induced cytoskeletal remodeling and migration in human olfactory GnRH-secreting neurons. Migrating GnRH neurons displayed up to a 3-fold increase in GnRH gene expression at the later stages of migration and at the point of entry into the developing forebrain (50). The significance of this increased GnRH production is not yet clear. It is possible that GnRH may activate pituitary gonadotropins during embryogenesis (51), thus playing a role in the organizational events of sexual differentiation (52, 53). This increase in GnRH expression may also be related to guiding the direction of other migratory cells to establish the neuronal network necessary for the functioning of the GnRH cell in the central nervous system (10). Although several genes appear to control the development of both the olfactory and GnRH system, factors that specified the onset of GnRH cell differentiation and the cues influencing the initial migratory phases out of the olfactory epithelium have not yet been determined. Recent research (54) has demonstrated that, in mouse, whereas GnRH cells differentiated from the nasal placode, nestin is identified in early expressing GnRH neurons and that cues of the midline nasal tissue down-regulated nestin. Because in FNC-B4 cells exposure to GnRH induced a decrease in nestin expression and an increase in GnRH expression, the lower nestin expression might be used as a marker for distinguishing those cells that diverge from the olfactory sensory lineage and are committed to becoming GnRH neurons. We have also hypothesized that GnRH in FNC-B4 cells might represent a specific signal for GnRH-neuroendocrine lineage differentiation and a cue for directed cell migration. A remarkable feature of olfactory neurons is that they have a half-life in the range of weeks and are replaced by new neurons that differentiate from a stem cell population present in the olfactory epithelium (55, 56). It is interesting to note that during adult life the olfactory epithelium retains the plasticity to generate not only olfactory neurons but also GnRH-secreting neurons. In fact, GnRH-secreting neurons are present in the nasal epithelium of both normal human fetuses and of normosmic eugonadal adult subjects (49, 57). We speculate that the nasal epithelium may be considered a reservoir for GnRH-secreting cells that may be activated under particular stimuli and that give rise to new neurons. Interruption of this hypothetical adult neurogenesis might account, at least in part, for the adult onset type of idiopathic hypogonadotropic hypogonadism. Thus, the ability of GnRH to induce differentiation and migration of human olfactory neuroblasts may have important clinical implications.

Acknowledgments—We gratefully acknowledge Dr. A. A. Karande (Department of Biochemistry, Indian Institute of Science, Bangalore, India) for generously providing the mouse MA to human pituitary GnRH-R (F1G4). We also thank Dr. Pietro Pantaleo for helpful supervision in statistical analysis.

REFERENCES

1. Schwanzel-Fukuda, M., and Pfaff, D. W. (1989) *Nature* **338,** 161–164
2. Wray, S., Grant, P., and Gainer, H. (1989) *Proc. Natl. Acad. Sci. U. S. A.* **86,** 8132–8136
3. Kramer, P. R., and Wray, S. (2000) *Genes Dev.* **14,** 1824–1834
4. Schwanzel-Fukuda, M., and Pfaff, D. W. (2002) *Prog. Brain Res.* **141,** 59–77
5. Mellon, P. L., Windle, J. J., Goldsmith, P. C., Padula, C. A., Roberts, J. L., and Weiner, R. I. (1990) *Neuron* **5,** 1–10
6. Radovick, S., Wray, S., Lee, E., Nicols, D. K., Nakayama, Y., Weintraub, B. D., Westphal, H., Cutler, G. B., Jr., and Wondisford, F. E. (1991) *Proc. Natl. Acad. Sci. U. S. A.* **88,** 3402–3406
7. Wetsel, W. (1995) *Cell. Mol. Neurobiol.* **15,** 43–78
8. Maggi, R., Pimpinelli, F., Molteni, L., Milani, M., Martini, L., and Piva, F. (2000) *Endocrinology* **141,** 2105–2112
9. Allen, M. P., Xu, M., Zeng, C., Tobet, S. A., and Wierman, M. E. (2000) *J. Biol. Chem.* **275,** 39662–39670
10. Wray, S. (2001) *J. Neuroendocrinol.* **13,** 3–11
11. Allen, M. P., Linseman, D. A., Udo, H., Xu, M., Schaack, J. B., Varnum, B., Kandel, E. R., Heidenreich, K. A., Wierman, M. E. (2002) *Mol. Cell Biol.* **22,** 599–613
12. Giacobini, P., Giampietro, C., Fioretto, M., Maggi, R., Cariboni, A., Perroteau, I., and Fasolo, A. (2002) *Endocrinology* **143,** 3306–3315
13. Rugarli, E. I., Lutz, B., Kuratani, S. C., Wawersik, S., Borsani, G., Ballabio, A., and Eichele, G. (1993) *Nat. Genet.* **4,** 19–26
14. Schwanzel-Fukuda, M., Bick, D., and Pfaff, D. W. (1989) *Mol. Brain Res.* **6,** 311–326
15. Nachtigall, L. B., Boepple, P. A., Pralong, F. P., and Crowley, W. F., Jr. (1997) *N. Engl. J. Med.* **336,** 410–415
16. Quinton, R., Cheow, H. K., Tymms, D. J., Bouloux, P. M., Wu, F. C., and Jacobs, H. S. (1999) *Clin. Endocrinol.* **50,** 481–485
17. Seminara, S. B., Oliveira, L. M., Beranova, M., Hayes, F. J., and Crowley, W. F., Jr. (2000) *J. Endocrinol. Invest.* **23,** 560–565
18. Oliveira, L. M., Seminara, S. B., Beranova, M., Hayes, F. J., Valkenburgh, S. B., Schipani, E., Costa, E. M., Latronico, A. C., Crowley, W. F., Jr., and Vallejo, M. (2001). *J. Clin. Endocrinol. Metab.* **86,** 1532–1538
19. MacColl, G., Quinton, R., and Bouloux, P. M. (2002) *Trends Endocrinol. Metab.* **13,** 112–118
20. Dode, C., Levilliers, J., Dupont, J. M., De Paepe, A., Le Du, N., Soussi-Yanicostas, N., Coimbra, R. S., Delmaghani, S., Compain-Nouaille, S., Baverel, F., Pecheux, C., Le Tessier, D., Cruaud, C., Delpech, M., Speleman, F., Vermeulen, S., Amalfitano, A., Bachelot, Y., Bouchard, P., Cabrol, S., Carel, J. C., Delemarre-van de Waal, H., Goulet-Salmon, B., Kottler, M. L., Richard, O., Sanchez-Franco, F., Saura, R., Young, J., Petit, C., and Hardelin, J. P. (2003) *Nat. Genet.* **33,** 463–465
21. Vannelli, G. B., Ensoli, F., Zonefrati, R., Kubota, Y., Arcangeli, A., Becchetti, A., Camici, G., Barni, T., Thiele, C. J., and Balboni, G. C. (1995) *J. Neurosci.* **15,** 4382–4394
22. Barni, T., Maggi, M., Fantoni, G., Granchi, S., Mancina, R., Gulisano, M., Marra, F., Macorsini, E., Luconi, M., Rotella, C., Serio, M., Balboni, G. C., and Vannelli, G. B. (1999) *J. Clin. Endocrinol. Metab.* **84,** 4266–4273
23. Maggi, M., Barni, T., Fantoni, G., Mancina, R., Pupilli, C., Luconi, M., Crescioli, C., Serio, M., and Vannelli, G. B. (2000) *J. Clin. Endocrinol. Metab.* **85,** 1658–1665
24. Florio, P., Vannelli, G. B., Luisi, S., Barni, T., Zonefrati, R., Falaschi, C., Bifulco, G., Genazzani, A. R., and Petraglia, F. (2000) *Eur. J. Endocrinol.* **143,** 133–138

25. Krsmanovic, L. Z., Stojilkovic, S. S., Balla, T., al-Damluji, S., Weiner, R, I., and Catt, K. J. (1991). *Proc. Natl. Acad. Sci. U. S. A.* **88,** 11124–11128
26. MacConell, L. A., Lawson, M. A., Mellon, P. L., and Roberts, V. J. (1999) *Neuroendocrinology* **70,** 246–254
27. Karande, A. A., Rajeshwari, K., Schol, D. J., and Hilgers, J. H. M. (1995) *Mol. Cell. Endocrinol.* **114,** 51–56
28. Peri, A., Dubin, N. H., Dhanireddy, R., and Mukherjee, A. B. (1995) *J. Clin. Invest.* **96,** 343–353
29. Bradford, M. M. (1976) *Anal. Biochem.* **72,** 248–254
30. Pinzani, M., Failli, P., Ruocco, C., Casini, A., Milani, S., Baldi, E., Giotti, A., and Gentilini, P. (1992) *J. Clin. Invest.* **90,** 642–646
31. Carloni, V., Romanelli, R. G., Pinzani, M., Laffi, G., and Gentilini, P. (1997) *Gastroenterology* **112,** 522–531
32. De Lean, A., Munson, P. J., Rodbard, D. (1978) *Am. J. Physiol.* **235,** E97–E102
33. Munson, P. J., and Rodbard, D. (1980) *Anal. Biochem.* **107,** 220–239
34. Limonta, P., Moretti, R. M., Marelli, M. M., Dondi, D., Parenti, M., and Motta, M. (1999) *Endocrinology* **140,** 5250–5256
35. Lendahl, U., Zimmerman, L, B., and McKay, R. D. (1990) *Cell* **60,** 585–595
36. Nunes, M. C., Roy, N. S., Keyoung, H. M., Goodman, R. R., McKhann, G., Jiang, L., Kang, J., Nedergaard, M., and Goldman, S. A. (2003) *Nat. Med.* **9,** 439–447
37. Sealfon, S. C., Weinstein, H., and Millar, R. P. (1997) *Endocr. Rev.* **18,** 180–205
38. Stojilkovic, S. S., Reinhart, J., and Catt, K. J. (1994) *Endocr. Rev.* **15,** 462–499
39. Krsmanovic, L. Z., Stojilkovic, S. S., Mertz, L. M., Tomic, M., and Catt, K. J. (1993) *Proc. Natl. Acad. Sci. U. S. A.* **90,** 3908–3912
40. Krsmanovic, L. Z., Martinez-Fuentes, A. J., Arora, K. K., Mores, N., Navarro, C. E., Chen, H. C., Stojilkovic, S. S., and Catt, K. J. (1999) *Endocrinology* **140,** 1423–1431
41. Stanislaus, D., Ponder, S., Ji, T. H., and Conn, P. M. (1998) *Biol. Reprod.* **59,** 579–586
42. Lin, X., and Conn, P. M. (1999) *Endocrinology* **140,** 358–364
43. Imai, A., Takagi, H., Horibe, S., Fuseya, T., and Tamaya, T. (1996) *J. Clin. Endocrinol. Metab.* **81,** 3249–3253
44. Grundker, C., Volker, P., and Emons, G. (2001) *Endocrinology* **142,** 2369–2380
45. Krsmanovic, L. Z., Mores, N., Navarro, C. E., Arora, K. K., and Catt, K. J. (2003) *Proc. Natl. Acad. Sci. U. S. A.* **100,** 2969–2974
46. Neves, S. R., Ram, P. T., and Iyengar, R. (2002) *Science* **296,** 1636–1639
47. Carlier, M. F., Clainche, C. L., Wiesner, S., and Pantaloni, D. (2003) *Bioessays* **25,** 336–345
48. Soussi-Yanicostas, N., de Castro, F., Julliard, A. K., Perfettini, I., Chedotal, A., and Petit, C. (2002) *Cell* **109,** 217–228
49. Kim, K. H., Patel. L., Tobet, S. A., King, J, C., Rubin, B. S., and Stopa, E. G. (1999) *Brain Res.* **826,** 220–229
50. Simonian, S. X., and Herbison, A. E. (2001) *Neuroendocrinology* **73,** 149–156
51. Salisbury, R. L., Dudley, S. D., and Weisz, J. (1982) *Neuroendocrinology* **35,** 265–269
52. Slob, A. K., Ooms, M. P., and Vreeburg, J. T. M. (1980) *J. Endocrinol.* **87,** 81–87
53. Aubert, M. L., Bégeot, M, Winiger, B. P., Moel, G., Sizonenko, P. C., and Dubois, P. M. (1985) *Endocrinology* **116,** 1565–1576
54. Kramer, P. R., and Wray, S. (2000) *Dev. Biol.* **227,** 343–357
55. Graziadei, P. P. C. (1973) *Tissue Cell* **5,** 113–131
56. Calof, A. L., and Chikaraishi, D. M. (1989) *Neuron* **3,** 115–127
57. Quinton, R., Hasan, W., Grant, W., Thrasivoulou, C., Quiney, R. E., Besser, G. M., and Bouloux, P. M. (1997) *J. Clin. Endocrinol. Metab.* **82,** 309–314

Expression and Function of Gonadotropin-releasing Hormone (GnRH) Receptor in Human Olfactory GnRH-secreting Neurons: AN AUTOCRINE GnRH LOOP UNDERLIES NEURONAL MIGRATION

Roberto Giulio Romanelli, Tullio Barni, Mario Maggi, Michaela Luconi, Paola Failli, Anna Pezzatini, Elisabetta Pelo, Francesca Torricelli, Clara Crescioli, Pietro Ferruzzi, Roberto Salerno, Mirca Marini, Carlo Maria Rotella and Gabriella B. Vannelli

J. Biol. Chem. 2004, 279:117-126.
doi: 10.1074/jbc.M307955200 originally published online October 16, 2003
